SUPPLEMENTAL MATERIAL

Abdelsamed et al., https://doi.org/10.1084/jem.20161760

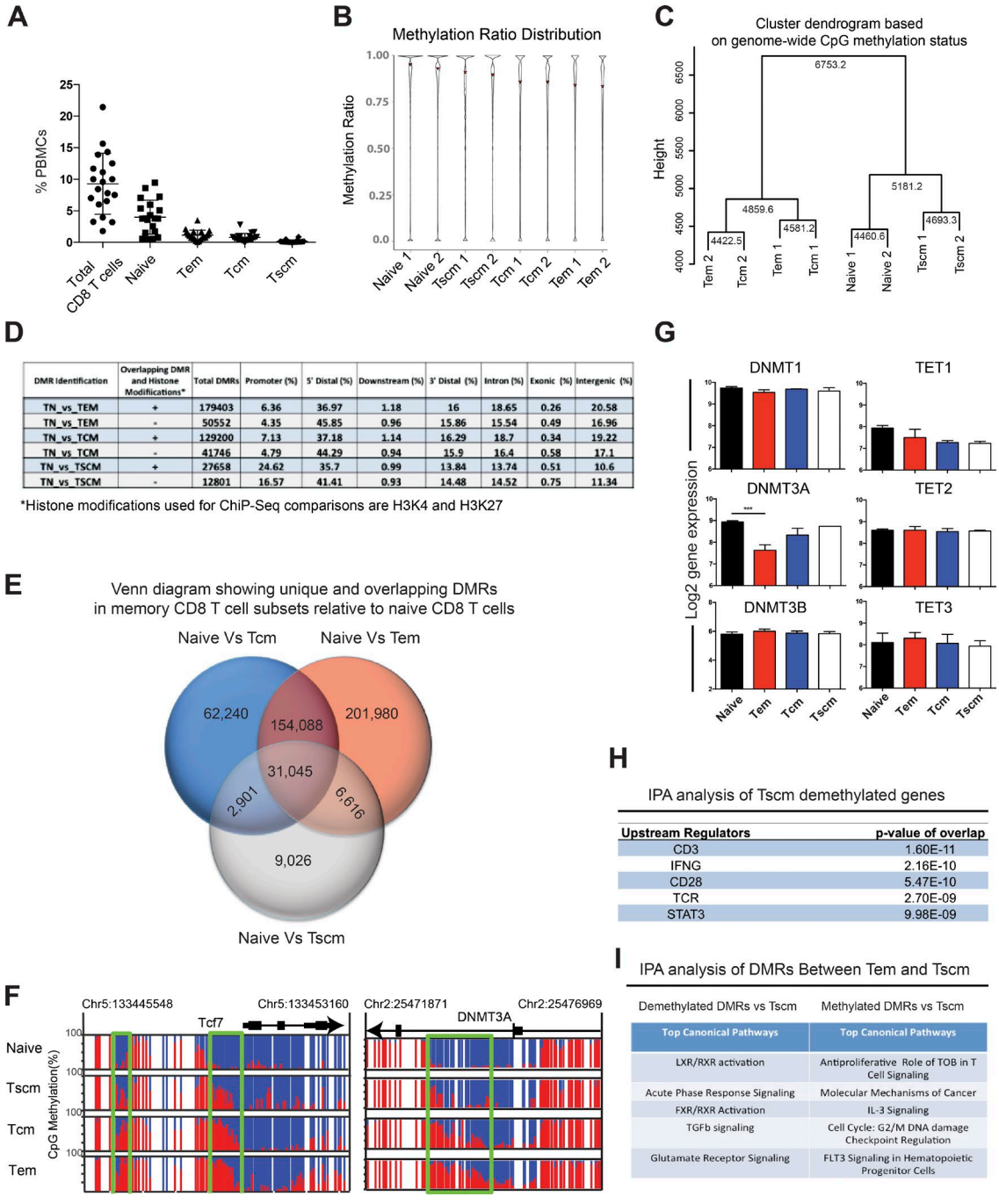

DMR Identification	Overlapping DMR and Histone Modifications*	Total DMRs	Promoter (%)	5' Distal (%)	Downstream (%)	3' Distal (%)	Intron (%)	Exonic (%)	Intergenic (%)
TN_vs_TEM	+	179403	6.36	36.97	1.18	16	18.65	0.26	20.58
TN_vs_TEM	-	50552	4.35	45.85	0.96	15.86	15.54	0.49	16.96
TN_vs_TCM	+	129200	7.13	37.18	1.14	16.29	18.7	0.34	19.22
TN_vs_TCM	-	41746	4.79	44.29	0.94	15.9	16.4	0.58	17.1
TN_vs_TSCM	+	27658	24.62	35.7	0.99	13.84	13.74	0.51	10.6
TN_vs_TSCM	-	12801	16.57	41.41	0.93	14.48	14.52	0.75	11.34

Demethylated DMRs vs Tscm	Methylated DMRs vs Tscm
LXR/RXR activation	Antiproliferative Role of TOB in T Cell Signaling
Acute Phase Response Signaling	Molecular Mechanisms of Cancer
FXR/RXR Activation	IL-3 Signaling
TGFb signaling	Cell Cycle: G2/M DNA damage Checkpoint Regulation
Glutamate Receptor Signaling	FLT3 Signaling in Hematopoietic Progenitor Cells

Figure S1. **Bioinformatics analyses of genome-wide naive and memory CD8 T cell DNA methylation datasets.** (A) Scatter plot showing the percentage of total CD8 T cells and naive and memory CD8$^+$ T cell subsets in human peripheral blood (n = 20 healthy donors). (B) Violin plots showing the methylation distribution (number of methylated CpGs per total number of CpGs) across the genomes of naive and memory CD8$^+$ T cell subsets from two donors. (C) Dendrogram of DMRs showing cluster analysis for two replicates for each cell population (naive, T_{EM}, T_{CM}, and T_{SCM} CD8 T cells). (D) Summary table of the percentage of overlap and relative genomic location between histone modifications and memory-associated DMRs. (E) Venn diagram showing the unique and overlapping DMRs in memory CD8 T cell subsets relative to naive CD8 T cells. (F) Normalized plot of CpG methylation at sites surrounding and within DMRs in the *DNMT3A* and *TCF7* loci obtained from WGBS analysis. Red and blue lines depict methylation and demethylation of CpG sites, respectively. (G) Log_2 gene expression data (means ± SEM) for DNMT and TET enzymes among naive and memory T cell subsets (n = 3 healthy donors) obtained from NCBI Gene Expression Omnibus database, submitted by Gattinoni et al. (2011). (H) Table of IPA analysis shows the upstream regulators of demethylated DMRs in T_{SCM} cells compared with those in naive CD8 T cells. (I) Table of IPA analyses shows the top canonical pathways of demethylated and methylated DMRs in T_{EM} cells compared with T_{SCM} CD8 T cells.

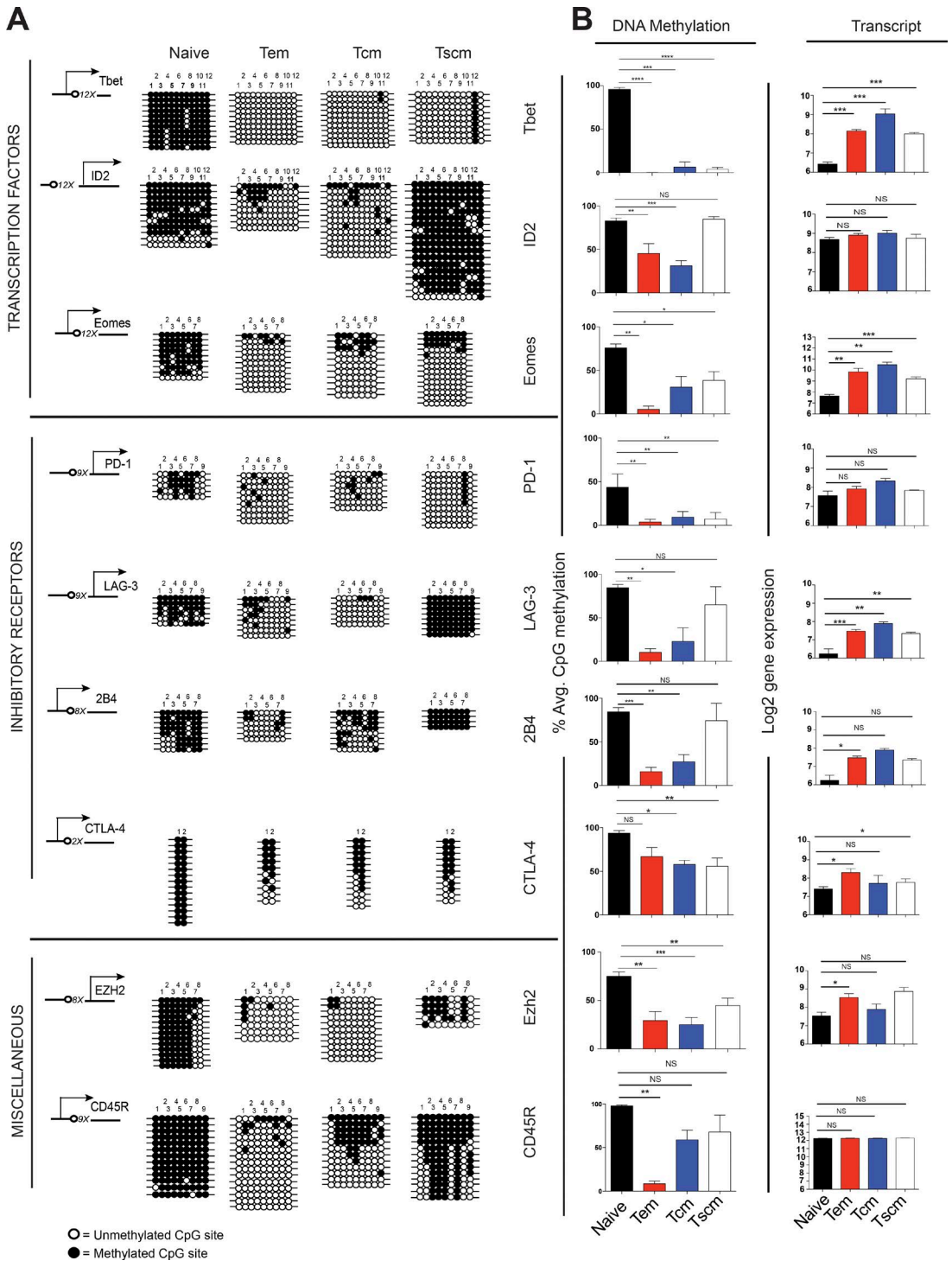

Figure S2. **Validation of unique differential methylation programming at memory and effector-associated loci in memory CD8 T cells.** (A) Representative bisulfite sequencing DNA methylation analysis of transcription factor loci (*T-BET*, *EOMES*, and *ID2*), inhibitory receptor loci (*PD-1*, *LAG-3*, *2B4*, and *CTLA-4*), histone methyltransferase *EZH2*, and *CD45R* tyrosine phosphatase (isoform C). Bisulfite sequencing was performed using genomic DNA from purified (>95% purity), naive, T_{EM}, T_{CM}, and T_{SCM} $CD8^+$ T cells. Black and white circles depict methylated and demethylated CpG sites, respectively. Each horizontal line represents a clone, whereas vertical lines represent CpG sites. (B) Bar graphs showing the mean percentage of CpG methylation (means ± SEM) for each locus (n = 3–6 healthy donors) and $\log_2$ gene expression data (means ± SEM) for each locus (n = 3 healthy donors) obtained from NCBI Gene Expression Omnibus database, submitted by Gattinoni et al. (2011). *, P < 0.05; **, P < 0.01; ***, P < 0.001; ****, P < 0.0001; considered significant using an unpaired Student's t test. NS, not significant.

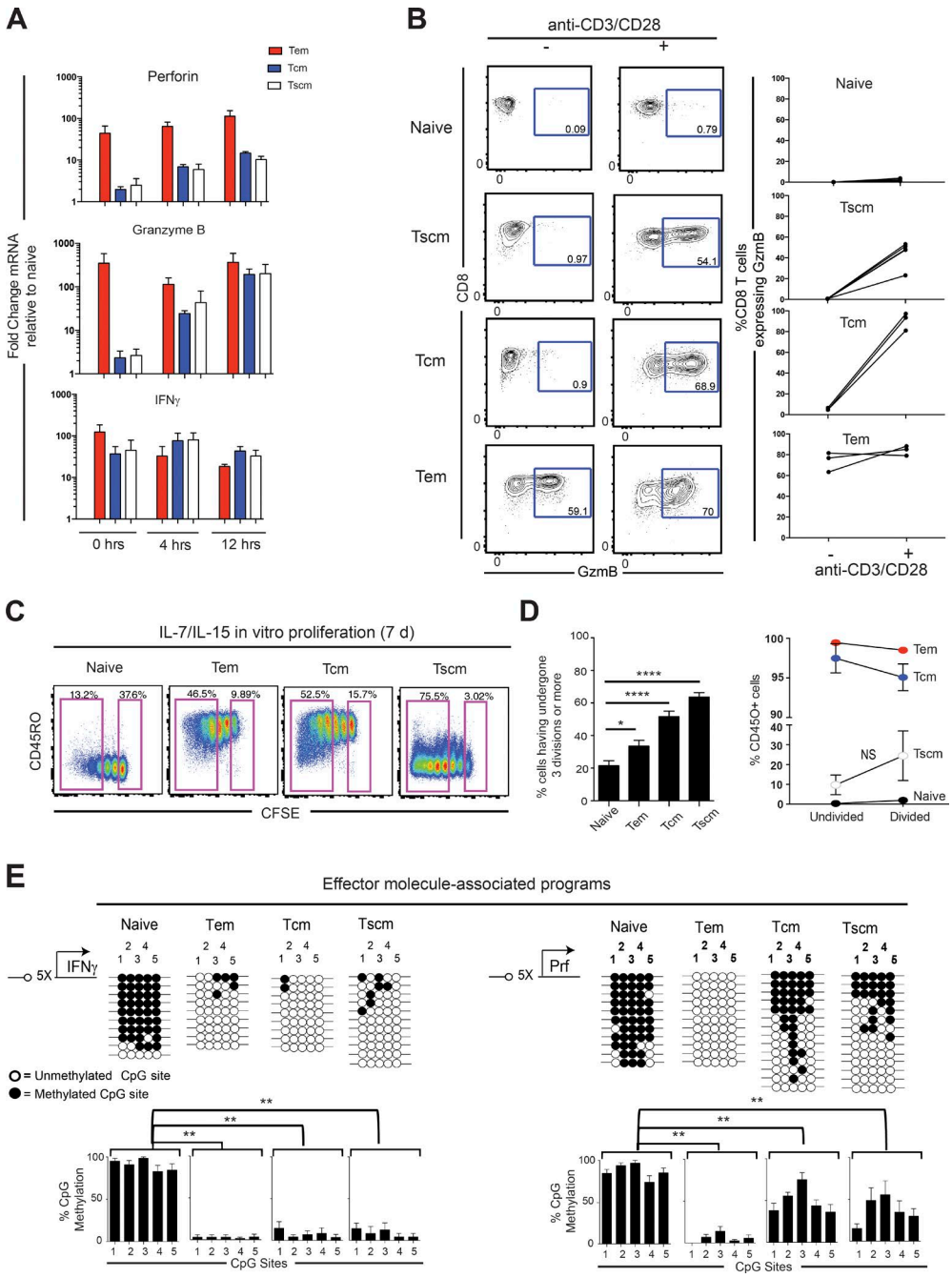

Figure S3. **Memory CD8 T cells are poised to elicit effector molecule expression.** (A) Expression kinetics of the transcripts encoding for *IFNγ*, *GZMB*, and *PRF1* at the indicated time points (0, 4, and 12 h) after anti-CD3/CD28 stimulation. Data represent mean relative expression ± SEM of three independent experiments. Values are calibrated against naive T cells at each time point. (B) GzmB intracellular expression levels after 18-h stimulation with anti-CD3/CD28 beads. Representative flow cytometric plots (left) and paired analysis (right) are shown. (C) CFSE dilution from one representative donor, showing proliferation of sorted CD8 T cell subsets after IL-7/IL-15 exposure in vitro for 7 d. The gates indicate the percentage of undivided cells and cells that have undergone three or more divisions. CD45RO expression in undivided and divided, CFSE-labeled, naive, T_{EM}, T_{CM}, and T_{SCM} CD8 T cells after exposure to IL-7/IL-15 in culture for 7 d. (D, left) Cumulative data from 12 independent experiments are presented as means ± SEM of highly proliferating cells (more than three divisions). *, $P < 0.05$; and ****, $P < 0.0001$ were considered significant using an unpaired Mann-Whitney *U* test. NS, not significant. (right) CD45RO expression. Paired Student's *t* test was used, and $P < 0.05$ was considered significant. NS, not significant. (E, top) DNA methylation profile analysis of the indicated IFNγ and Prf1 DMRs in ex vivo isolated CD8 T cell subsets from one representative donor. Each horizontal line represents a clone, and each vertical represents a CpG site. (bottom) Bar graphs showing the percentage of CpG methylation (means ± SEM) for each site (n = 5–6 healthy donors). Mann-Whitney *U* test was used. **, $P < 0.005$ was considered significant. NS, not significant. Statistical comparison was based on the mean value of all CpG sites.

REFERENCE

Gattinoni, L., E. Lugli, Y. Ji, Z. Pos, C.M. Paulos, M.F. Quigley, J.R. Almeida, E. Gostick, Z. Yu, C. Carpenito, et al. 2011. A human memory T cell subset with stem cell-like properties. *Nat. Med.* 17:1290–1297. http://dx.doi.org/10.1038/nm.2446